

A Comprehensive Approach to Unsupervised Embedding Learning based on AND Algorithm

Sungwon Han¹, Yizhan Xu², Sungwon Park¹,
Meeyoung Cha^{3,1}, and Cheng-Te Li²

¹ School of Computing, KAIST

² Institute of Data Science, National Cheng Kung University

³ Data Science Group, Institute for Basic Science

Abstract. Unsupervised embedding learning aims to extract good representation from data without the need for any manual labels, which has been a critical challenge in many supervised learning tasks. This paper proposes a new unsupervised embedding approach, called Super-AND, which extends the current state-of-the-art model [11]. Super-AND has its unique set of losses that can gather similar samples nearby within a low-density space while keeping invariant features intact against data augmentation. Super-AND outperforms all existing approaches and achieves an accuracy of 89.2% on the image classification task for CIFAR-10. We discuss the practical implications of this method in assisting semi-supervised tasks.

Keywords: Unsupervised embedding learning · Computer vision

1 Introduction

Unsupervised embedding learning aims to extract visually meaningful representations without any label information. Here “visually meaningful” refers to finding features that satisfy two traits: (1) positive attention and (2) negative separation [21,30]. Data samples from the same class (i.e., positive samples) should be close to one another in the embedding space. In contrast, those from different classes (i.e., negative samples) should be positioned far away from each other. This task is challenging in unsupervised learning since a model does not know a priori which data points are positive or negative.

Several innovative approaches have been proposed. The sample specificity approach starts by assuming all data points to be negative samples and separates them in the feature space [27,3]. This approach, however, suffers from a bias that the learning process relies solely on negative separation. The data augmentation approach, in contrast, considers positive samples in training [30]. This new approach efficiently reduces the ambiguity in supervision while keeping invariant features in the embedding space. More recently, the anchor neighborhood discovery (AND) method has been proposed, which alleviates the complexity in boundaries by progressively discovering the nearest neighbor among the data

points [11]. These methods each tackle the different limitations of the sample specificity approach. However, no unified approach exists.

This paper presents a holistic method for unsupervised embedding learning, named Super-AND. It extends the AND [11] algorithm and unifies the merits of previous methods with its unique architecture. Our model not only focuses on learning distinctive features across neighborhoods but also utilizes the edge information in embeddings to maintain the invariant class properties in data augmentation. The model also newly introduces the Unification Entropy loss (UE-loss), an adversary of the sample specificity loss that is critical in gathering similar data points within a low-density space. Extensive experiments on several benchmark datasets verify the superiority of Super-AND. The main contributions of this paper are as follows:

- We propose a comprehensive model, Super-AND, which unifies some of the key techniques from existing research and introduces a novel loss (UE-loss) that gathers similar samples in a low-density space.
- For the image classification task, Super-AND outperforms all baselines with an accuracy of 89.2% in CIFAR-10 with the ResNet18 backbone network, which is a 2.9% gain over the state-of-the-art.
- The ablation study shows that every component of Super-AND contributes to the performance increase and that their synergy is critical.
- Super-AND can further improve better-understood tasks like semi-supervised learning when used in the pre-training step.

The outstanding performance of Super-AND is a step closer to the broader adoption of unsupervised techniques in computer vision tasks. The premise of “data-less embedding learning” is at its applicability to practical scenarios, where there exists only one or two examples per cluster. Codes and training data from this research are accessible via the github link⁴.

2 Related Work

Existing studies can be summarized into four groups.

Generative model. This type of model is a powerful branch in unsupervised learning. By reconstructing data based on its underlying distribution, a model can generate new data points as well as features without label supervision. Generative adversarial networks (GAN) [8] have led rapid progress in image generation problems [1,32]. Several studies have utilized GAN for unsupervised embedding learning [22]. However, the main objective of generative models lies at mimicking the true distribution of each class, rather than discovering distinctive categorical information the data contains.

Self-supervised learning. This type of learning uses inherent structures in images as pseudo-labels and exploits labels for back-propagation. For example,

⁴ <https://github.com/super-AND/super-AND>

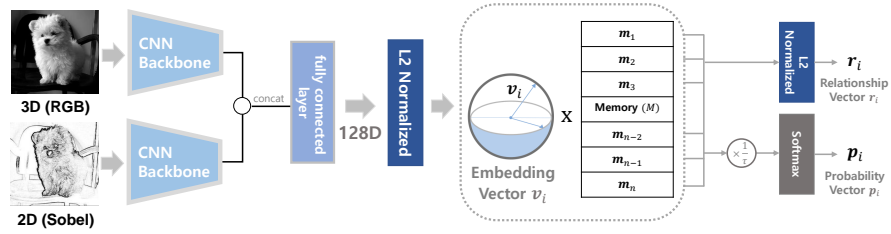


Fig. 1: Illustration of basic architecture in Super-AND.

a model can be trained to create embeddings by predicting the relative position of a pixel from other pixels [6] or the degree of changes after rotating images [7]. Predicting future frames of a video can benefit from this technique [25]. All of these methods are suitable for unsupervised embedding learning, although there exists a risk of false knowledge from generated labels that weakly correlate with the underlying class information.

Sample-specificity learning. This type of model learns feature representation from capturing apparent discriminability among instances. By considering all instances as a single individual class, they trained the classifier to separate data points in a confined space [3,27]. This learning method holds because a deep learning model can detect the similarity through supervised learning. However, its decision boundary becomes complex when the number of classes gets larger.

Clustering analysis. This type of analysis is an extensively studied area in unsupervised learning, whose main objective is to group similar objects into the same class. Many studies either leverage deep learning for dimensionality reduction before clustering [23,2] or train models in an end-to-end fashion [28,29]. Deep cluster [4] is an iterative method that updates its weights by predicting cluster assignments as pseudo-labels. However, directly reasoning the global structures without any label is known to be error-prone. The AND model [11], which we extend in this study, combines the advantages of the sample specificity approach and the clustering method to mitigate any noisy supervision via neighborhood analysis.

3 The Super-AND Model

Problem definition. Assume that we are given an unlabeled image set \mathcal{I} , and a batch set \mathcal{B} with n images: $\mathcal{B} = \{\mathbf{x}_1, \mathbf{x}_2, \dots, \mathbf{x}_n\} \subset \mathcal{I}$. The goal of unsupervised embedding learning is to obtain a feature extractor f_θ whose generated representations (i.e., $\mathbf{v}_i = f_\theta(\mathbf{x}_i)$) are “visually meaningful,” a definition we discussed earlier.

Let $\hat{\mathcal{B}} = \{\hat{\mathbf{x}}_1, \hat{\mathbf{x}}_2, \dots, \hat{\mathbf{x}}_n\}$ be the augmentation set of input batches \mathcal{B} . Super-AND projects images $\mathbf{x}_i, \hat{\mathbf{x}}_i$ from batches $\mathcal{B}, \hat{\mathcal{B}}$ to 128-dimensional embeddings $\mathbf{v}_i, \hat{\mathbf{v}}_i$. During this process, the Sobel-processed images [18] are used, and the feature

vectors from both images are concatenated to emphasize the edge information in embeddings (i.e., see the left side in Fig. 1). Concatenated vectors are projected to 128-dimensional sphere embeddings with L2 normalization, and these are treated as latent representations of given images.

Similar to the sample specificity learning [3,27], our model considers every data sample as an independent class at first. The model computes the probability \mathbf{p}_i^j of the i -th image being recognized as the j -th class. Since every instance is a prototype of its class, the similarity between instance i and class j becomes a dot product of feature vectors $(\mathbf{v}_i, \mathbf{v}_j)$ from two images \mathbf{x}_i and \mathbf{x}_j . By applying the softmax function, we can calculate \mathbf{p}_i . We denote the superscript j in vector notation as the j -th component value of a given vector. (Eq. 1).

$$P(j|\mathbf{v}_i) = \mathbf{p}_i^j = \frac{\exp(\mathbf{v}_j^\top \mathbf{v}_i)}{\sum_{k=1}^n \exp(\mathbf{v}_k^\top \mathbf{v}_i)} \quad (1)$$

Calculating embedding from all images (i.e., \mathbf{v}_k) in every iteration loop is computationally demanding. To reduce such complexity, we set up a memory bank M to save an instance embedding \mathbf{m}_i accumulated from the previous steps, as proposed in [27]. For every iteration, the i -th instance’s embedding vector \mathbf{m}_i in memory bank M is updated by the exponential moving average [17], taking into account the latest embedding vector \mathbf{v}_i (Eq. 2). With the help of embedding \mathbf{m}_i in the memory, the lightweight version of \mathbf{p}_i can be calculated as in Eq. 3. The temperature parameter ($\tau < 1$) is added to ensure a label distribution with low entropy [10].

$$\mathbf{m}_i = (1 - \eta) \cdot \mathbf{m}_i + \eta \cdot \mathbf{v}_i \quad (2)$$

$$P(j|\mathbf{v}_i) = \mathbf{p}_i^j = \frac{\exp(\mathbf{m}_j^\top \mathbf{v}_i / \tau)}{\sum_{k=1}^n \exp(\mathbf{m}_k^\top \mathbf{v}_i / \tau)} \quad (3)$$

$$\mathbf{r}_i^j = \frac{\mathbf{v}_i \cdot \mathbf{m}_j}{\|\mathbf{v}_i\| \cdot \|\mathbf{m}_j\|}, \quad \hat{\mathbf{r}}_i^j = \frac{\hat{\mathbf{v}}_i \cdot \mathbf{m}_j}{\|\hat{\mathbf{v}}_i\| \cdot \|\mathbf{m}_j\|} \quad (4)$$

To detect any discrepancy after data augmentation, we define the relationship vectors $\mathbf{r}_i, \hat{\mathbf{r}}_i$ through the cosine similarity between the embedding vectors of original images and their augmented versions $(\mathbf{v}_i, \hat{\mathbf{v}}_i)$, and the memory bank M (Eq. 4). Using \mathbf{p}, \mathbf{v} , and \mathbf{r} , we construct three losses: the AND-loss (L_{and}), the UE-loss (L_{ue}), and the AUG-loss (L_{aug}). The proposed model is finally trained by optimizing L_{total} with the hyper-parameter $w(t)$ that controls the weights of UE-loss (Eq. 5). Below we describe each loss function.

$$L_{total} = L_{and} + w(t) \times L_{ue} + L_{aug} \quad (5)$$

3.1 The AND-loss: Neighborhood discovery and supervision loss

Existing clustering methods [4,28] train networks to find an optimal mapping. However, their learning process is unstable due to random initialization and

overfitting [31]. The newly proposed Anchor Neighbourhood Discovery (AND) method suggests a finer-grained clustering that gradually discovers ‘neighborhoods’ [11]. By considering the nearest-neighbor pairs as local classes, AND can separate data points that belong to different neighborhood sets from those in the same neighborhood set. We adopt this novel discovery strategy for Super-AND.

The AND algorithm has three main steps: (1) neighborhood discovery, (2) progressive neighborhood selection with curriculum, and (3) neighborhood supervision. For the first step, the k nearest neighborhood (k -NN) algorithm is used to discover all neighborhoods (Eq. 6 and Eq. 7). When k is set to 1, each neighborhood constructs the pair of two nearest data points.

$$\tilde{\mathcal{N}}(\mathbf{x}) = \{\mathbf{x}_i | \mathbf{x}_i \neq \mathbf{x}, f_\theta(\mathbf{x}_i)^\top f_\theta(\mathbf{x}) \text{ is top-}k \text{ in } \mathcal{I}\} \quad (6)$$

$$\tilde{\mathcal{N}} = \{(\mathbf{x}_i, \tilde{\mathcal{N}}(\mathbf{x}_i)) | \mathbf{x}_i \in \mathcal{I}\} \quad (7)$$

The neighbor pairs are then progressively selected for curriculum learning over multiple rounds. Every round, the model gradually increases the number of discovered neighborhoods for training. The key here is to keep the discovery of multiple class “consistent” clusters, where its progressive nature helps provide a consistent view of local class information at each round during training.

Selecting candidate neighborhoods for local classes rely on the entropy of probability vector $H(\mathbf{x}_i)$ (Eq. 8). Probability vector \mathbf{p}_i , obtained from the softmax function (Eq. 3), represents the visual similarity between training instances in a probabilistic manner. Data points with low entropy represent that they reside in a relatively low-density area and have only a few surrounding neighbors. Neighborhood pairs containing such data points tend to share consistent and easily distinguishable features, compared to other pairs. AND selects neighborhood set \mathcal{N} from $\tilde{\mathcal{N}}$ that is in a lower entropy order. Data points that are not selected belong to the complement set \mathcal{N}^c .

$$H(\mathbf{x}_i) = - \sum_j \mathbf{p}_i^j \log \mathbf{p}_i^j \quad (8)$$

The AND-loss distinguishes neighborhood pairs from one another. Data points from the same neighborhoods need to be classified in the same class (i.e., the left-hand term in Eq. 9). As for the remaining data points that are not chosen, each forms an independent class (i.e., the right-hand term in Eq. 9).

$$L_{and} = - \sum_{i \in (\mathcal{B} \cap \mathcal{N})} \log \left(\sum_{j \in \{\mathbf{x}_i, \tilde{\mathcal{N}}(\mathbf{x}_i)\}} \mathbf{p}_i^j \right) - \sum_{i \in (\mathcal{B} \cap \mathcal{N}^c)} \log \mathbf{p}_i^i \quad (9)$$

3.2 The UE-loss: Unification entropy loss

Existing sample specificity methods [27,3] consider every data point as a prototype for a class. They use the cross-entropy loss to separate all data points in the L2-normalized embedding space. Due to the confined space, data points cannot be placed far away from one another, and similar samples are located nearby.

The unification entropy loss aims to strengthen the concentration-effect above. We define it as the entropy of the probability vector $\tilde{\mathbf{p}}_i$. Probability vector $\tilde{\mathbf{p}}_i$ is calculated from the softmax function, and this represents the similarity between instances except for every instance itself (Eq. 10). By excluding the self-class, minimizing this loss leads nearby data points to approach each other even more aggressively. This idea is contrary to minimizing the sample specificity loss. Employing both the AND-loss and the UE-loss will enforce similar neighborhoods to be positioned close while keeping the overall neighborhoods as separated as possible. This loss is calculated as in Eq. 11.

$$\tilde{\mathbf{p}}_i^j = \frac{\exp(\mathbf{m}_j^\top \mathbf{v}_i / \tau)}{\sum_{k=1, k \neq i}^n \exp(\mathbf{m}_k^\top \mathbf{v}_i / \tau)} \quad \tilde{H}(\mathbf{x}_i) = - \sum_{j \neq i} \tilde{\mathbf{p}}_i^j \log \tilde{\mathbf{p}}_i^j \quad (10)$$

$$L_{ue} = \sum_i \tilde{H}(\mathbf{x}_i) \quad (11)$$

3.3 The AUG-loss: Data augmentation loss

Data augmentation is one of the unsupervised methods to learn which features are substantial [12,30]. The premise of this method lies in the assumption that simple augmentation does not deform the underlying data characteristic. Then, invariant features learned from the augmented data should still contain class-relevant information, and hence a training network will show performance gain.

The augmentation loss represents invariant image features. Assume the model inspects an original data image and its augmented variants, then all augmented instances are viewed as positive samples. The relationship vectors \mathbf{r}_i (Eq. 4), which show the similarity between all instances stored in the memory, should also be similar to the initial data points, compared to those from other instances in the same batch. In Eq. 12, the probability of an augmented instance that is correctly identified as class- i is denoted as $\tilde{\mathbf{p}}_i^i$; and that of i -th original instance that is falsely identified as class- j ($j \neq i$), $\tilde{\mathbf{p}}_i^j$. The augmentation loss is then defined to minimize any misclassification over instances in all batches (Eq. 13).

$$\tilde{\mathbf{p}}_i^i = \frac{\exp(\mathbf{r}_i^\top \hat{\mathbf{r}}_i / \tau)}{\sum_{k=1}^n \exp(\mathbf{r}_k^\top \hat{\mathbf{r}}_i / \tau)} \quad \tilde{\mathbf{p}}_i^j = \frac{\exp(\mathbf{r}_j^\top \mathbf{r}_i / \tau)}{\sum_{k=1}^n \exp(\mathbf{r}_k^\top \mathbf{r}_i / \tau)}, \quad j \neq i \quad (12)$$

$$L_{aug} = - \sum_i \sum_{j \neq i} \log(1 - \tilde{\mathbf{p}}_i^j) - \sum_i \log(\tilde{\mathbf{p}}_i^i) \quad (13)$$

4 Experiments

We first enumerate the Super-AND model with different backbone networks on both coarse-grained and fine-grained benchmarks. Our ablation study helps speculate which components of the model are critical. We also compare the proposed model with the original AND, which our Super-AND extended from. Finally, we test Super-AND’s potential to assist in semi-supervised learning tasks.

4.1 Implementation details

Datasets. A total of six datasets were utilized. Three are coarse-grained: (1) *CIFAR-10* [14] has 10-class images of 32×32 pixels. (2) *CIFAR-100* contains images in CIFAR-10 and has 100 classes. (3) *SVHN* [19] (Street View House Numbers) is a real-world dataset of 10-class images of 32×32 pixels. The other three are fine-grained: (4) *Stanford Dogs (SD)* [13] contains dog images of 120 breeds, (5) *CUB-200* [26] is from Caltech containing bird images of 200 species, and (6) *STL-10* [5] contains 10-class images of 96×96 pixels such as airplanes and birds. The last dataset (6) is used only for qualitative analysis.

Training. We used AlexNet [15] and ResNet18 [9] as backbone networks. Hyperparameters were tuned in the same manner as in the AND paper [11] unless explicitly mentioned. We used SGD with Nesterov momentum 0.9 for the optimizer. We fixed the learning rate as 0.03 for the first 80 epochs, and scaled-down by 0.1 every 40 epochs. Neighborhood size k for AND-loss was set to 1, the batch size to 128, and the model was trained in 5 rounds and 200 epochs per round. Weights for the UE-loss $w(t)$ (Eq 5) were initialized from 0 and increased by 0.2 every 80 epochs. For the Aug-loss, we used four types: Resized Crop, Grayscale, ColorJitter, and Horizontal Flip. Horizontal Flip was not used in the case of the SVHN dataset because this dataset includes digit images. Update momentum η of the exponential moving average for memory bank was set to 0.5.

Evaluation. Following the method from [27], we used the weighted k -NN algorithm for an image classification task. Top k -nearest neighbors \mathcal{N}_{top} were retrieved and used to predict the final outcome in a weighted fashion. We set $k = 200$ and the weight function for each class c as $\sum_{i \in \mathcal{N}_{top}} \exp(\mathbf{v}_i^\top M / \tau) \cdot \mathbf{1}(c_i = c)$ with $\tau = 0.07$, where c_i is the class index for i -th instance. Top-1 classification accuracy was used for evaluation.

4.2 Results & Component analysis

Baseline models. We adopt the following six competitive baselines for comparison: (1) *Split-Brain* [33], (2) *Counting* [20], (3) *DeepCluster* [4], (4) *Instance* [27], (5) *ISIF* [30], and (6) *AND* [11], which also used the same backbone networks.

Coarse-grained evaluation. Table 1 describes the image classification performance of seven models, including the proposed Super-AND on three coarse-grained datasets: CIFAR-10, CIFAR-100, and SVHN. Super-AND outperforms competitive baselines on all datasets except for one case; ISIF performs the best on CIFAR-100 with AlexNet. For all other cases, Super-AND performs the best. We notice that the performance gain is larger when ResNet18 is used as the neural network architecture than for AlexNet. This finding indicates that Super-AND brings more substantial advantage for stronger CNN architectures such as ResNet18.

Table 1: k -NN Evaluation on coarse-grained datasets. Results marked as * are borrowed from the previous work [11,30].

Dataset (Network)	CIFAR-10		CIFAR-100		SVHN	
	ResNet18	AlexNet	ResNet18	AlexNet	ResNet18	AlexNet
Split-Brain*	-	11.7	-	1.3	-	19.7
Counting*	-	41.7	-	15.9	-	43.4
DeepCluster*	67.6	62.3	-	22.7	-	84.9
Instance	80.8	60.3	50.7	32.7	93.6	79.8
ISIF	83.6	74.4	54.4	44.1	91.3	89.8
AND	86.3	74.8	57.2	41.5	94.4	90.9
Super-AND	89.2	75.6	61.5	42.7	94.9	91.9

Table 2: k -NN evaluation on fine-grained datasets.

Dataset	SD	CUB-200
Instance	27.0	11.6
ISIF	31.4	13.2
AND	32.3	14.4
Super-AND	39.0	17.6

Table 3: Backbone test on CIFAR-10.

Network	Accuracy
AlexNet	75.6
ResNet18	89.2
ResNet101	90.5

Table 4: Ablation study on CIFAR-10.

Network	Accuracy
Full	89.2
Without UE	88.7
Without Aug	88.5
Without Sobel	88.3

Fine-grained evaluation. The examination on fine-grained datasets requires the ability to discriminate subtle differences across classes. Table 2 shows that Super-AND outperforms the competitors by a large margin on more challenging fine-grained recognition tasks. We excerpted results for Instance and AND from existing studies, and the backbone network was ResNet18.

Backbone network. The choice of the backbone neural network architecture affects the overall performance. Test of AlexNet, ResNet18, and ResNet101 on the CIFAR-10 dataset, shown in Table 3, reveals that our method performs better under stronger networks. This implies the possibility for an even higher gain under future neural network architectures.

Ablation study. To examine the compactness, we removed each of the following components in turn and compared the full Super-AND model along with the following variants: (1) without the unification entropy loss, (2) without the Sobel filter, (3) without the augmentation loss. Table 4 displays the evaluation results based on the CIFAR-10 dataset and the ResNet18 backbone network. Every component is shown to contribute to the performance increase. Among the three, the largest performance gain is observed from the Sobel filter that is used for edge detection by removing color information in images.

4.3 Comparison to the AND model

Embedding quality analysis. We investigated the embedding quality by evaluating the class consistency of selected neighborhoods. Cheat labels are used to

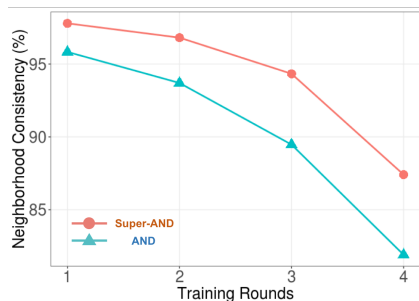


Fig. 2: Neighborhood consistency over training rounds.

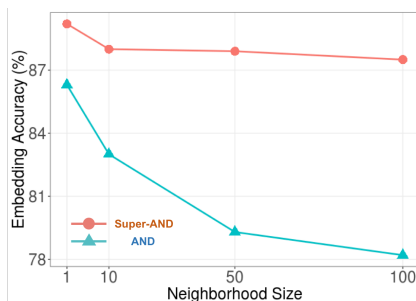


Fig. 3: Effect of neighborhood size k to embedding accuracy.

check whether neighborhood pairs come from the same class. Since both algorithms increase the selection ratio every round when gathering the part of discovered neighborhoods, the consistency of selected neighborhoods will naturally decrease. This relationship is drawn in Fig. 2. The reduction, in contrast, is less significant for Super-AND; our model maintains high-performance throughout the training rounds.

We evaluated the effect of neighborhood size k in both algorithms (Eq. 6). Neighborhood size controls the number of data points within each cluster, and thus, the labeling consistency of each cluster is affected by this hyper-parameter. Generally, a bigger neighborhood produces poorer results due to the noise from a wider set of images as well as initial randomness. However, Fig. 3 shows that Super-AND model is robust to such noise even when neighborhood size reaches to a large value (i.e., $k = 100$).

Qualitative study. Fig. 4 illustrates the top-5 nearest retrievals of AND (i.e., upper rows) and Super-AND (i.e., lower rows) based on the STL-10 dataset. The example queries show dump trucks, airplanes, horses, and monkeys. Red framed images, which indicate negative samples (or wrong class labels), appear more frequently for AND than Super-AND. Clusters in Super-AND are robust to misleading color information and better recognizing the object shapes. For example, in the ‘Airplane’ query, pictures retrieved from Super-AND are consistent in shape, whereas the AND result falsely includes a cruise picture. Also, in other examples, Super-AND is more flexible in allowing various colored objects such as a red dump truck or a spotted horse.

4.4 Application to semi-supervised learning

As a practical application, we demonstrate the potential for Super-AND to be used as a pre-training step for well-known semi-supervised learning tasks. We empirically confirm the usefulness by comparing the performance of several sole baseline algorithms (Supervised, H -model [16], and Mean-Teacher [24]) and that of the same algorithms with pre-trained by the proposed model. ‘Supervised’ in this experiment refers to using only labeled data to train the neural network.



Fig. 4: The nearest-neighbor retrievals of example queries from STL-10. The upper retrieval row from every query shows the results from AND, and the lower ones are from Super-AND. The left-side results are successful cases for both models, and the right-side results are failure cases. Images with surrounding red frames indicate the wrongly retrieved negative samples.

Table 5: Accuracy on 4000 labeled CIFAR-10. Semi-supervised learning with pre-trained network achieves improved performance. (*II* : *II*-model, MT : Mean-Teacher)

Dataset	Supervised	<i>II</i>	MT	Supervised (our)	<i>II</i> (our)	MT (our)
CIFAR-10	79.65	83.76	84.23	84.72	85.23	87.63

CIFAR-10 with 4000 labels is selected for evaluation, and WideResNet28-2 is selected as a backbone network in all algorithms for a fair comparison. A breakthrough of performance is reported in Table 5 for all three cases, implying that semi-supervised learning with pre-trained Super-AND can be a practical approach for leveraging both unlabeled and labeled data when labels are scarce.

5 Conclusion

This paper presented Super-AND, a comprehensive technique for unsupervised learning of deep embedding, which showed excellent potential for common computer vision tasks. Super-AND combines advantages of the existing techniques (i.e., sample specificity, clustering, anchor neighborhood discovery, data augmentation), and newly proposes a novel loss (UE-loss) that collects nearby data points nearby even in a low-density space. This method excelled in image classification tasks with both coarse-grained and fine-grained datasets, against all existing models. Implications of this research are enormous; as deep embedding learning advances, unsupervised learning approaches becomes an economically viable option in scenarios where labels are costly to generate. Our method can further assist the current semi-supervised tasks when used in the pre-training step.

References

1. Martin Arjovsky, Soumith Chintala, and Léon Bottou. Wasserstein generative adversarial networks. In *Proc. of the International conference on machine learning*, pages 214–223, 2017.
2. Pierre Baldi. Autoencoders, unsupervised learning, and deep architectures. In *Proc. of the ICML workshop on unsupervised and transfer learning*, pages 37–49, 2012.
3. Piotr Bojanowski and Armand Joulin. Unsupervised learning by predicting noise. In *Proc. of the International Conference on Machine Learning-Volume 70*, pages 517–526. JMLR. org, 2017.
4. Mathilde Caron, Piotr Bojanowski, Armand Joulin, and Matthijs Douze. Deep clustering for unsupervised learning of visual features. In *Proc. of the European Conference on Computer Vision*, pages 132–149, 2018.
5. Adam Coates, Andrew Ng, and Honglak Lee. An analysis of single-layer networks in unsupervised feature learning. In *Proc. of the international conference on artificial intelligence and statistics*, pages 215–223, 2011.
6. Carl Doersch, Abhinav Gupta, and Alexei A Efros. Unsupervised visual representation learning by context prediction. In *Proc. of the IEEE International Conference on Computer Vision*, pages 1422–1430, 2015.
7. Spyros Gidaris, Praveer Singh, and Nikos Komodakis. Unsupervised representation learning by predicting image rotations. *arXiv preprint arXiv:1803.07728*, 2018.
8. Ian Goodfellow, Jean Pouget-Abadie, Mehdi Mirza, Bing Xu, David Warde-Farley, Sherjil Ozair, Aaron Courville, and Yoshua Bengio. Generative adversarial nets. In *Proc. of the Advances in neural information processing systems*, pages 2672–2680, 2014.
9. Kaiming He, Xiangyu Zhang, Shaoqing Ren, and Jian Sun. Deep residual learning for image recognition. In *Proc. of the IEEE conference on computer vision and pattern recognition*, pages 770–778, 2016.
10. Geoffrey Hinton, Oriol Vinyals, and Jeff Dean. Distilling the knowledge in a neural network. *arXiv preprint arXiv:1503.02531*, 2015.
11. Jiabo Huang, Qi Dong, Shaogang Gong, and Xiatian Zhu. Unsupervised deep learning by neighbourhood discovery. In *Proc. of the International Conference on Machine Learning*, pages 2849–2858, 2019.
12. Xu Ji, Joo F. Henriques, and Andrea Vedaldi. Invariant information clustering for unsupervised image classification and segmentation. *arXiv preprint arXiv:1807.06653*, 2018.
13. Aditya Khosla, Nityananda Jayadevaprakash, Bangpeng Yao, and Li Fei-Fei. Novel dataset for fine-grained image categorization. In *Proc. of the First Workshop on Fine-Grained Visual Categorization, IEEE Conference on Computer Vision and Pattern Recognition*, Colorado Springs, CO, June 2011.
14. Alex Krizhevsky et al. Learning multiple layers of features from tiny images. Technical report, Citeseer, 2009.
15. Alex Krizhevsky, Ilya Sutskever, and Geoffrey E Hinton. Imagenet classification with deep convolutional neural networks. In *Proc. of the Advances in neural information processing systems*, pages 1097–1105, 2012.
16. Samuli Laine and Timo Aila. Temporal ensembling for semi-supervised learning. *arXiv preprint arXiv:1610.02242*, 2016.
17. James M Lucas and Michael S Saccucci. Exponentially weighted moving average control schemes: properties and enhancements. *Technometrics*, 32(1):1–12, 1990.

18. Raman Maini and Himanshu Aggarwal. Study and comparison of various image edge detection techniques. *International journal of image processing*, 3(1), 2008.
19. Yuval Netzer, Tao Wang, Adam Coates, Alessandro Bissacco, Bo Wu, and Andrew Y Ng. Reading digits in natural images with unsupervised feature learning, 2011.
20. Mehdi Noroozi, Hamed Pirsiavash, and Paolo Favaro. Representation learning by learning to count. In *Proc. of the IEEE International Conference on Computer Vision*, pages 5898–5906, 2017.
21. Hyun Oh Song, Yu Xiang, Stefanie Jegelka, and Silvio Savarese. Deep metric learning via lifted structured feature embedding. In *Proc. of the IEEE Conference on Computer Vision and Pattern Recognition*, pages 4004–4012, 2016.
22. Alec Radford, Luke Metz, and Soumith Chintala. Unsupervised representation learning with deep convolutional generative adversarial networks. In *Proc. of the International Conference on Machine Learning*, 2016.
23. Florian Schroff, Dmitry Kalenichenko, and James Philbin. Facenet: A unified embedding for face recognition and clustering. In *Proc. of the IEEE conference on computer vision and pattern recognition*, pages 815–823, 2015.
24. Antti Tarvainen and Harri Valpola. Mean teachers are better role models: Weight-averaged consistency targets improve semi-supervised deep learning results. In *Advances in Neural Information Processing Systems*, pages 1195–1204, 2017.
25. Jacob Walker, Carl Doersch, Abhinav Gupta, and Martial Hebert. An uncertain future: Forecasting from static images using variational autoencoders. In *Proc. of the European Conference on Computer Vision*, pages 835–851, 2016.
26. P. Welinder, S. Branson, T. Mita, C. Wah, F. Schroff, S. Belongie, and P. Perona. Caltech-UCSD Birds 200. Technical Report CNS-TR-2010-001, California Institute of Technology, 2010.
27. Zhirong Wu, Yuanjun Xiong, Stella X Yu, and Dahua Lin. Unsupervised feature learning via non-parametric instance discrimination. In *Proc. of the IEEE Conference on Computer Vision and Pattern Recognition*, pages 3733–3742, 2018.
28. Junyuan Xie, Ross Girshick, and Ali Farhadi. Unsupervised deep embedding for clustering analysis. In *Proc. of the International conference on machine learning*, pages 478–487, 2016.
29. Jianwei Yang, Devi Parikh, and Dhruv Batra. Joint unsupervised learning of deep representations and image clusters. In *Proc. of the IEEE Conference on Computer Vision and Pattern Recognition*, pages 5147–5156, 2016.
30. Mang Ye, Xu Zhang, Pong C Yuen, and Shih-Fu Chang. Unsupervised embedding learning via invariant and spreading instance feature. In *Proc. of the IEEE Conference on Computer Vision and Pattern Recognition*, pages 6210–6219, 2019.
31. Dejiao Zhang, Yifan Sun, Brian Eriksson, and Laura Balzano. Deep unsupervised clustering using mixture of autoencoders. *arXiv preprint arXiv:1712.07788*, 2017.
32. Han Zhang, Ian Goodfellow, Dimitris Metaxas, and Augustus Odena. Self-attention generative adversarial networks. In *Proc. of the International Conference on Machine Learning*, pages 7354–7363, 2019.
33. Richard Zhang, Phillip Isola, and Alexei A Efros. Split-brain autoencoders: Unsupervised learning by cross-channel prediction. In *Proc. of the IEEE Conference on Computer Vision and Pattern Recognition*, pages 1058–1067, 2017.